Available online at www.sciencedirect.com
ScienceDirect
Chinese Journal of Natural Medicines 2019, **17**(1): 0003−0014
Chinese Journal of Natural Medicines

•Special topic•

An insoluble polysaccharide from the sclerotium of *Poria cocos* improves hyperglycemia, hyperlipidemia and hepatic steatosis in *ob*/*ob* mice *via* modulation of gut microbiota

SUN Shan-Shan [1, 2], WANG Kai [2, 3], MA Ke [2, 3], BAO Li [2, 3], LIU Hong-Wei [2, 3*]

[1] *School of Life Sciences, University of Science and Technology of China, Hefei 230026, China;*
[2] *State Key Laboratory of Mycology, Institute of Microbiology, Chinese Academy of Sciences, Beijing 100101, China;*
[3] *University of Chinese Academy of Sciences, Beijing, 100049, China*

Available online 20 Jan., 2019

[ABSTRACT] Metabolic syndrome characterized by obesity, hyperglycemia and liver steatosis is becoming prevalent all over the world. Herein, a water insoluble polysaccharide (WIP) was isolated and identified from the sclerotium of *Poria cocos*, a widely used Traditional Chinese Medicine. WIP was confirmed to be a (1-3)-*β*-D-glucan with an average Mw of 4.486×10^6 Da by NMR and SEC-RI-MALLS analyses. Furthermore, oral treatment with WIP from *P. cocos* significantly improved glucose and lipid metabolism and alleviated hepatic steatosis in *ob/ob* mice. 16S DNA sequencing analysis of cecum content from WIP-treated mice indicated the increase of butyrate-producing bacteria *Lachnospiracea*, *Clostridium*. It was also observed that WIP treatment elevated the level of butyrate in gut, improved the gut mucosal integrity and activated the intestinal PPAR-*γ* pathway. Fecal transplantation experiments definitely confirmed the causative role of gut microbiota in mediating the benefits of WIP. It is the first report that the water insoluble polysaccharide from the sclerotium of *P. cocos* modulates gut microbiota to improve hyperglycemia and hyperlipidemia. Thereby, WIP from *P. cocos,* as a prebiotic, has the potential for the prevention or cure of metabolic diseases and may elucidate new mechanism for the efficacies of this traditional herbal medicine on the regulation of lipid and glucose metabolism.

[KEY WORDS] *Poria cocos*; Water insoluble polysaccharide; Metabolic syndrome; Prebiotics; Gut microbiota

[CLC Number] R965 **[Document code]** A **[Article ID]** 2095-6975(2019)01-0003-12

Introduction

Recent survey showed rapidly increased prevalence of the metabolic syndrome among individuals all over world. Metabolic syndrome is characterized with several factors, including insulin resistance, central obesity, high blood pressure, dyslipidemia and hyperglycemia. Furthermore, Gut microbiota, a complex ecosystem composing of approximately 1200 species in the human gastrointestinal tract, is well established as one important factor involved in the regulation of glucose and lipid metabolism. The modulation of gut microbiota is a novel therapeutic strategy for control of metabolic syndrome, such as obesity, diabetes and nonalcoholic fatty live disease (NAFLD) [1-4].

The prebiotic refers to non-digestible dietary ingredients that are able to generate the beneficial changes in the gut microbiota. A number of experiments and clinical applications have confirmed prebiotics can promote gastroenterological balance and improve host health. Nowadays, polysaccharides from mushrooms have attracted much attention due to their property of modulating gut microbiota as prebiotics. The polysaccharide from *Ganoderma lucidum* was reported to reduce body weight, inflammation, and insulin resistance in high-fat diet (HFD) induced-obesity mice *via* decreasing of the Firmicutes-to-Bacteroidetes ratios and endotoxin-bearing Proteobacteria levels [5]. The polysaccharide from *Inonotus obliquus* was found to ameliorate chronic pancreatitis by regulation of gut microbiota composition and diversity [6]. The polysaccharide of *Hericium erinaceus* was demonstrated to possess clinical potential in relieving inflammatory bowel

[Received on] 1-Oct.-2018
[Research funding] This work was supported by the National Key R&D program of China (No. 2018YFD0400203), the Strategic Biological Resources Service Network programme of CAS and Key Research Program of the Chinese Academy of Sciences (No. KFZD-SW-219) and the Youth Innovation Promotion Association of CAS (No. 2014074).
[*Corresponding author] Tel: 86-10-64806074, E-mail: liuhw@im.ac.cn (LIU Hong-Wei)
These authors have no conflict of interest to declare.

disease (IBD) by the enrichment of the anti-inflammatory microbes such as *Bifidobacterium*, *Parabacteroids*, *Lactobacillus* and the reduction of pro-inflammatory microbes such as *Corynebacterium*, *Staphylococcus* and *Sutterella* [7].

The sclerotium of *Poria cocos* is used as a traditional Chinese medicine to treat chronic gastritis, acute gastroenteric, gastric atony, edema, nephrosis, dizziness and emesis. *P. cocos* is also consumed as a health-promoting food in China and believed to have beneficial effects on food absorption and metabolism. Polysaccharides and triterpenes were reported to be the main bioactive ingredients of *P. cocos*. In this study, we isolated and identified a water insoluble polysaccharide (WIP) from the sclerotium of *P. cocos.* The water insoluble polysaccharides from *P. cocos* have not been investigated for its potential in improving metabolic disorders and modulating the gut microbiota. Experiments with *ob/ob* mice indicated that WIP treatment significantly improved glucose and lipid metabolism, reduced the inflammation and hepatic steatosis through modulating the gut microbiota. The increase of butyrate-producing bacteria in gut microbiota together with the following recovery of gut mucosal integrity contributes to metabolic benefits of WIP. It is for the first time that this water insoluble polysaccharide from the sclerotium of *P. cocos* was confirmed to improve hyperglycemia and hyperlipidemia via modulation of gut micriobiota.

Materials and Methods

Preparation and analysis of polysaccharide

The sclerotium of *P. cocos* was collected from Yunnan province and identified by Prof. ZHAO Rui-Lin from Institute of Microbiology, Chinese Academy of Sciences. The dried sclerotium of *P. cocos* (250 g) was ground into powder and extracted four times with ethanol (1.75 L) by Soxhelt extraction to remove lipid-soluble molecules. The residue (228.1 g) was extracted twice with distilled water (1.25 L) at 100 °C for 3 hours to remove water soluble polysaccharides. Finally, the residue (213.3 g) was extracted with 0.75 mol·L^{-1} NaOH (4 L) for 4 hours. The obtained supernatant was neutralized with dilute hydrochloric acid to afford the polysaccharides precipitate. The precipitate obtained by centrifugation (5000 rpm, 10 min) was repeatedly washed with bulk mass distilled water to remove water-soluble impurities and salts. The precipitate (10 g) suspended in 300 mL water was further dialyzed in a 100 kDa molecular weight cut off dialysis bag with flowing distilled water for 12 hours. Finally, a total of 99.5 g water insoluble polysaccharide (WIP) was obtained from *P. cocos* after lyophilization.

The structural characteristics of WIP were analysis by HPLC, IR, UV and NMR. IR data was recorded on a Nicolet IS5FTIR spectrophotometer using the KBr-disk method. UV data was measured using a Thermo Genesys-10S UV-vis spectrophotometer. NMR spectra were acquired with Bruker Avance-500 spectrometer and WIP was dissolved in DMSO-d_6. The monosaccharide composition was analyzed after 1-phenyl-3-methyl-5-pyrazolne (PMP)-derivatization. First, the solution of WIP (5 mg) in 2 mL 6 mol·L^{-1} HCl was heated at 110 °C for 4 h to hydrolysis. The resulting solution was then evaporated and subjected to derivatization according to the reported method [8]. After derivation, the sample was analyzed by HPLC using Phenomenex Gemini 5μm C18 110A column with a flow rate of 0.8 ml·min^{-1}. Standard monosaccharide was derivative in the same way. HPLC analysis condition: solvent A, MeCN; solvent B, water with 1% methane acid; linear gradient: 0−35 min, 75%−100% B in A. The Molecular weight of WIP was determined by SEC coupled with MALLS Dawn DSP detector and a refractive index (RI) detector (Wyatt Technology) using Shodex OH pack SB-806 HQ as the chromatographic separation column. The polysaccharide was dissolved in 0.5 mol·L^{-1} NaOH aqueous solution (concentration: 5 mg·mL^{-1}). The inject volume of sample was 20 μL. The column was eluted with water at a flow rate of 0.75 ml·min^{-1}. The value of dn/dc was 0.138 mL·g^{-1} during the calculation of molecular.

Animals and animal care

All procedures were performed in accordance to the standards of the Department of Health and Human Services, and under protocols approved by the 'regulation' of the Institute of Microbiology, Chinese Academy of Sciences (IMCAS) of Research Ethics Committee (permit APIMCAS2017023). Care and husbandry followed standard guidelines. C57BL/6J and *ob/ob* mice (8 weeks old) were purchased from the Experimental Animal Center, Chinese Academy of Medical Sciences. During one week of acclimatization, animals were housed 5/cage under controlled conditions of temperature and humidity, on a 12 h light/dark cycle with free access to normal chow and water.

Animals were sorted into five groups (n = 10 each) based on their blood glucose levels and body weight. WIP-treated groups were given with WIP (1.0 g·kg^{-1}, 0.5 g·kg^{-1}) daily by gavage. Inulin-treated group was given with inulin (5.0 g·kg^{-1}). The model group (*ob/ob* mice) and control group (C57BL/*6J* mice) were treated with an oral gavage of an equivalent volume of water. Treatments were continued for 4 weeks. Body weight, free diet blood glucose and blood glucose after 4h fasting were measured weekly. At the end of the study, mice were anesthetized by diethyl ether (Beijing Chemical Works, Beijing, China) and blood was sampled from the portal and cava veins. Subcutaneous adipose tissue depots, intestines and liver were precisely dissected, weighed, immersed immediately in liquid nitrogen, and stored at −80 °C for further analysis.

Oral glucose tolerance test (OGTT) and insulin tolerance test (ITT)

OGTT was performed by oral administration of a glucose bolus (2 g·kg^{-1}) after overnight fasting at 25th day. ITT was performed by injecting insulin (0.6 U·kg^{-1}) intraperitoneally after a 4-hour fasting at 27th day. The level of blood glucose was measured using a glucose meter (Accu Check, Roche, Switzerland) before oral glucose load (0 min) and at 30, 60, and 120 min after treating. The area under the curves (AUCs)

generated from the data collected during the ITT or OGTT was calculated by Graphpad 6.0.

Biochemical analyses

Serum total cholesterol (TC), triglycerides (TG), low density lipoprotein cholesterol (LDL-C), superoxide dismutase (SOD) measured by a commercial kit (Nanjing Jianchen Bioengineering Institute, Jiangsu, China). Serum insulin and tumor necrosis factor (TNF)-α concentrations were performed using a commercial ELISA kit (HuaBoDeYi, Beijing, China). Serum LPS quantification was determined using a commercial kit based on the use of a Limulus amaebocyte extracts (YEASEN, Shanghai, China). The insulin sensitivity index (ISI) was calculated from the values of fasting blood glucose (FBG, in $mg \cdot dL^{-1}$) and fasting blood insulin (FBI, in $mU \cdot L^{-1}$). ISI = 1/1000 (FBG × FBI). The liver homogenate of 10% *W/V* was prepared from the fresh liver tissue and physiological saline. Then, the homogenate was centrifuged at 3000 rpm for 10 min at 4 °C. The supernatant was carried on for further analysis. Hepatic total cholesterol (TC), triglycerides (TG), low density lipoprotein cholesterol (LDL-C) was quantified with above commercially available kit. The level of nitrate in the ileum was determined by the Griess assay as described previously [9].

Histological analysis

Samples of liver and abdominal white adipose tissue (WAT) were resected and fixed in 10% formaldehyde, followed by dehydration, embedding in paraffin, sectioning and staining with haematoxylin/esosin (H&E stain) as described previously [9].

Quantitative real-time PCR

Total RNA was extracted from the liver and ileum tissue with the TRIzol reagent according to the manufacturer's protocol (Invitrogen, Carlsbad, CA, USA). Reverse transcription was performed on 1μg of total RNA using a cloned AMV first-strand cDNA synthesis kit (Tiangen, Beijing, China). Primers used for cDNA amplification by real-time PCR are listed in Table 1. Glyceraldehyde-3-phosphate dehydrogenase (GAPDH) was used as the housekeeping gene for normalization of the target genes expression. PCR reactions were performed using Perfecta SYBR green super mix (KAPA).

Table 1 Primers used in this study

Name	Sequence (5'→ 3')
Gapdh-forward	AGGTCGGTGTGAACGGATTTG
Gapdh-reverse	TGTAGACCATGTAGTTGAGGTCA
Muc5-forward	GTGGTTTGACACTGACTTCCC
Muc5-reverse	CTCCTCTCGGTGACAGAGTCT
Occludin-forward	TTGAAAGTCCACCTCCTTACAGA
Occludin-reverse	CCGGATAAAAAGAGTACGCTGG
ZO-1-forward	ACCCGAAACTGATGCTGTGGATAG
ZO-1-reverse	AAATGGCCGGGCAGAACTTGTGTA
Pparg-forward	CCCAGGCCGGAGTTTAACC
Pparg-reverse	GTTGCTCATAAAGTCGGTGCT

Gut microbiota analysis

Total DNA was isolated from cecum content, sequencing the variable V3 and V4 regions of the 16S rRNA gene was performed with the Illumina HiSeq PE250 platform. The 16S rRNA gene V3-V4 region was amplified using the primers F341 (CCTA CGGGRSGCAGCAG) and R806 (GGACTAC VVGGGTAT CTAATC). The overlapping paired-end reads were merged using fastq-join and processed with QIIME. Only Illumina reads with an average score greater than 20 were retained for further analysis. The reads were checked with Chimera and assigned to operational taxonomic units (OTUs) with a 97% similarity threshold. Data analyses were performed by a previously reported method [10].

SCFA analyses

SCFA concentrations in feces were analyzed by gas chromatography-mass spectrometry (GC-MS) method [10]. In brief, 40 mg freeze-drying fecal sample was diluted in 1 mL methanol mixed thoroughly and centrifuged. The supernatant was subjected by GC-MS analysis. GC-MS was performed on a GCMS-QP2010 Ultra with an autosampler (SHIMADZU) and the Rtx-wax capillary column (60 m, 0.25 mm i.d., 0.25 μm film thickness; SHIMADZU). Oven temperature was programmed from 60 to 100 ºC at 5 ºC·min^{-1}, with a 1 min hold; to 150 ºC at 5 ºC·min^{-1}, with a 5 min hold; to 225 ºC at 30 ºC·min^{-1}, with a 20 min hold. Injection of a 2μL sample was performed at 230 ºC. Helium, at a flow of 1.2 mL· min^{-1}, was used as the carrier gas. Electronic impact was recorded at 70 eV.

Fecal transplantation

Fecal microbiota transplantation was performed based on a previously reported method [5]. 8-week-old male *ob/ob* mice were fed with WIP-H for 4 weeks. After 2 weeks feeding, stools were collected daily and immersed immediately in liquid nitrogen, and stored at –80 °C. Stools from mice were pooled and 100 mg was resuspended in 1 mL of sterile saline. The solution was vigorously mixed before centrifugation at 800 g for 3 min. The supernatant was collected and used as transplantation material. Fresh transplantation material was prepared on the same day of transplantation within 10 min

before oral gavage to prevent changes in bacterial composition. Eight-week-old male *ob/ob* mice were inoculated daily with fresh transplantation material (100 ml for each mouse) by oral gavage for 3 weeks.

Statistical analysis

For all analyses and for each group, any exclusion decision was made according to results obtained by the Grubbs test for outlier detection. All results are expressed as mean ± SEM. Statistical analysis was performed using two-way ANOVA followed by the Tukey's multiple comparison tests with GraphPad 6.0 for multiple comparisons. $P < 0.05$ was considered statistically significant.

Results

Structural characterization of WIP

WIP was obtained with a yield of about 39.8% from the sclerotium of *P. cocos*. High-performance size exclusion chromatography analysis of WIP indicated a single homogeneous composition with Mw mass of 4.486×10^6 Da and Mn mass of 4.031×10^5 Da, respectively. The Fourier transform infrared spectrum (FT-IR) spectrum of WIP showed the absorptions at 3395, 2914, 1200-1000 cm^{-1}, corresponding to the vibration of O-H, C-H, C-O, C-O-C bonds, respectively. The absorptions at 1074 and 890 cm^{-1} suggested a pyranose form of sugars with β anomeric configuration. The monosaccharide composition of the polysaccharide was determined as D-glucose by acid hydrolysis followed with HPLC analysis of the corresponding derivatives (Fig. 1). The ^1H, ^{13}C NMR, HSQC and ^1H-^1H COSY spectra of WIP, confirmed the main chain of WIP to be 1,3-β-D-glucan on the basis of the signals observed at 103.1/ 4.51 (d, J = 7.5 Hz, H-1), 72.8/3.26 (H-2), 86.4/3.44(H-3), 68.4/3.19(H-4), 76.3/3.26 (H-5), 60.9/3.68, 3.44(H-6) [11].

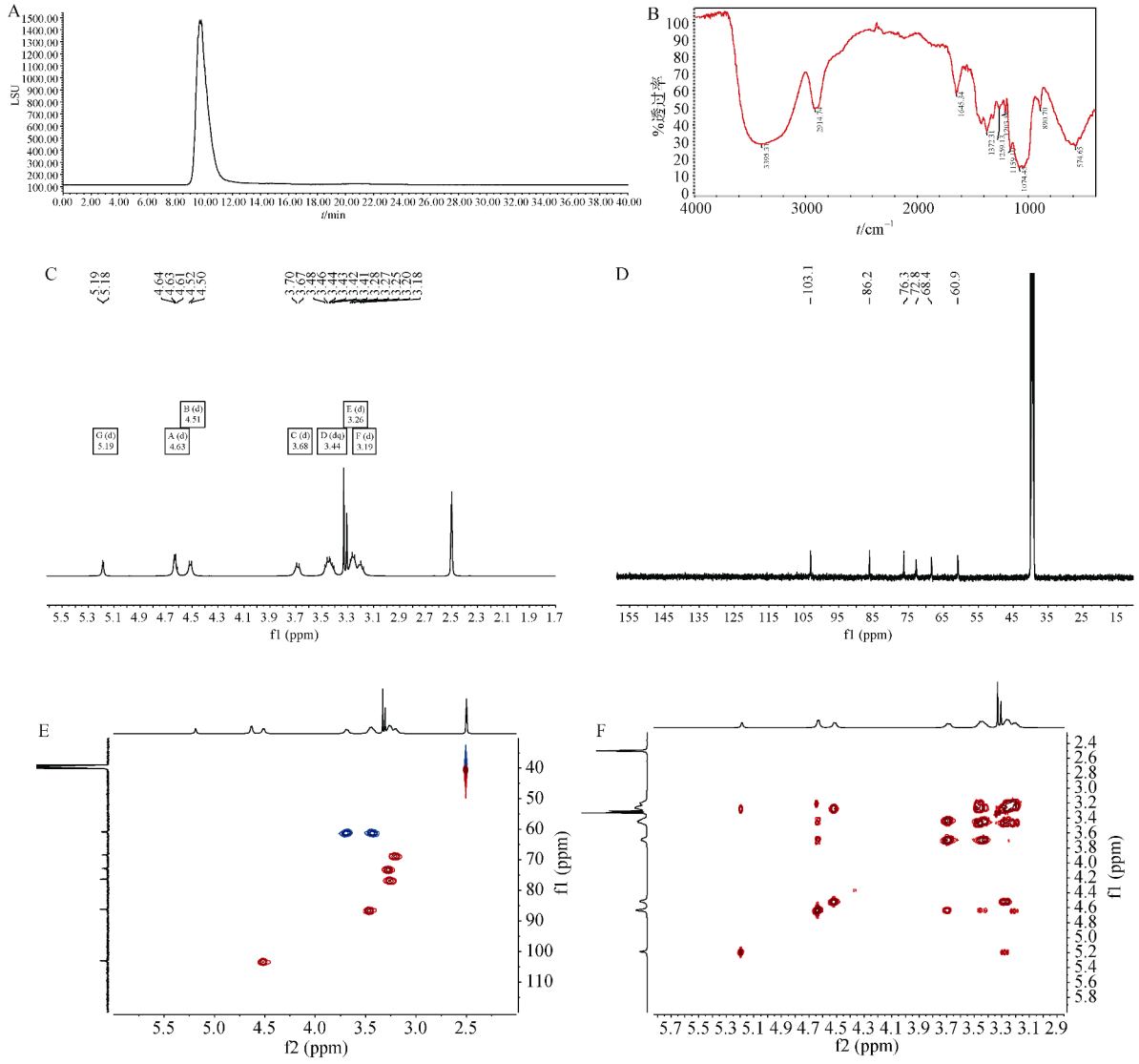

Fig. 1 Structural characterization of WIP. (A) HPGPC of WIP, (B) FT-IR spectrum of WIP, (C) ^1H spectrum of WIP in DMSO-d_6, (D) ^{13}C spectrum of WIP in DMSO-d_6, (E) ^1H-^1H COSY spectrum of WIP in DMSO-d_6, (F) HMBC spectrum of WIP in DMSO-d_6

WIP treatment ameliorates hyperglycemia and insulin resistance

We used *ob/ob* mice to evaluate the hypoglycemic and hypolipidemic effects for WIP. Inulin, a widely used prebiotic with multiple benefits on metabolic syndrome *via* the mediation of gut microbiota, was used as positive control [12-13]. WIP (1.0 g·kg^{-1}, 0.5 g·kg^{-1}) was daily administered by oral gavage for a period of 4 weeks.

It was observed that WIP (at 1.0 g·kg^{-1} and 0.5 g·kg^{-1}) significantly reduced both fasted blood glucose and free diet blood glucose after 7-day treatment (Figs. 2A−B). Glycosylated hemoglobin A1c (HbA1c), a gold indicator for the glucose level in clinic [14], was reduced substantially (Fig. 2C). WIP treatment also improved glucose tolerance and insulin resistance. The mean area under curves (AUC) during the oral glucose tolerance test (OGTT) and the insulin tolerance test (ITT) of APS-treated *ob/ob* mice was much lower than that of the vehicle-treated *ob/ob* mice (Figs. 2D−G). WIP treatment at the dose of 1.0 g·kg^{-1} and 0.5 mg·kg^{-1} also caused elevation of 49% and 33% in the ISI levels of *ob/ob* mice, respectively, as compared with that of the model group (Fig 2I). In contrast, the positive control of inulin exhibited little effects on glucose tolerance and insulin resistance.

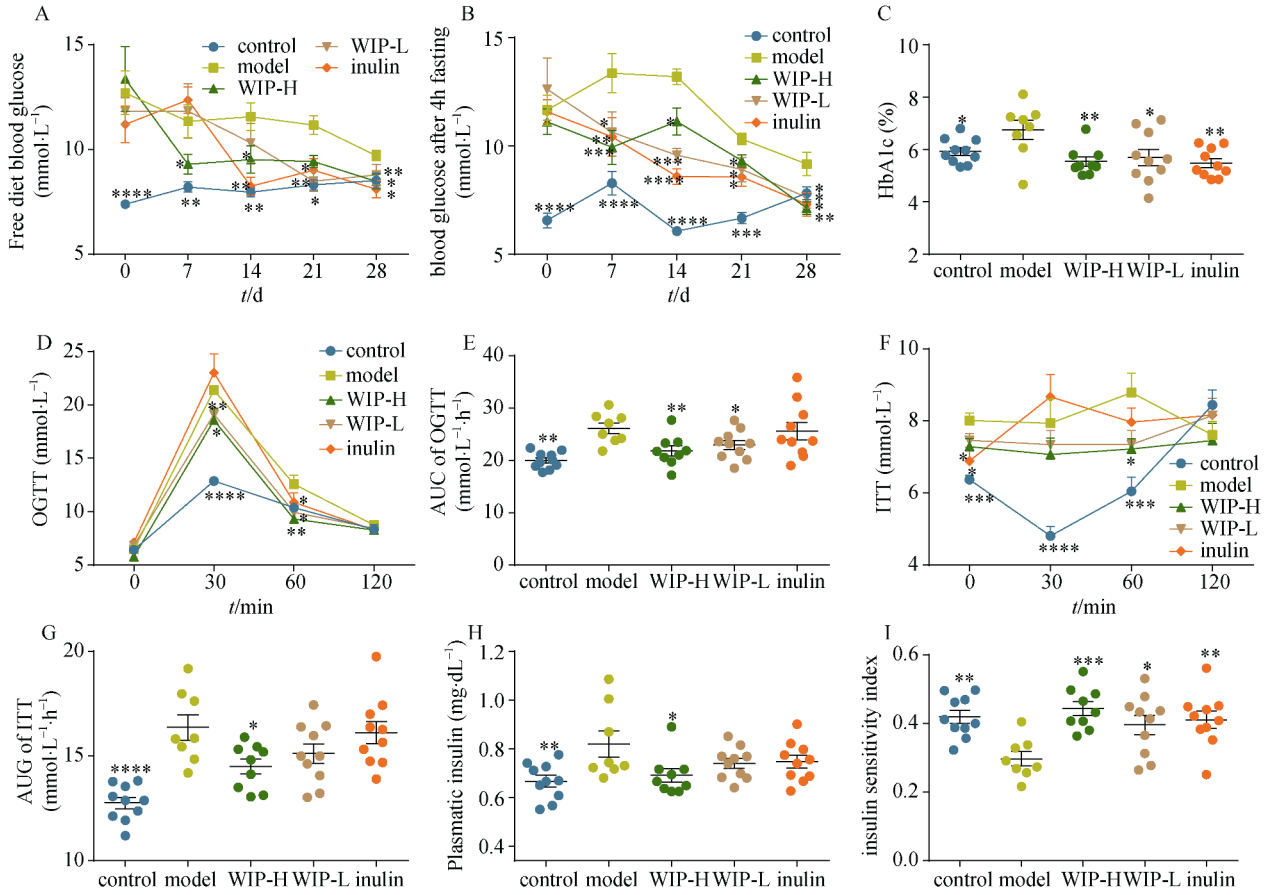

Fig. 2 Effects of WIP on blood glucose level and insulin resistance. (A) Free diet glucose; (B) Blood glucose after 4h fasting; (C) HbA1c in *ob/ob* mice; (D) OGTT and (E) AUC on the 25th day of treatment; (F) ITT and (G) AUC on the 27th day of treatment; (H) Plasmatic insulin, (I) Insulin sensitivity index (ISI). Control, C57B6/*J* mice control; Model, *ob/ob* model; WIP-H, WIP 1.0 g·kg^{-1}; WIP-L, WIP 0.5 g·kg^{-1}; Insulin, Insulin 5.0 g·kg^{-1}. Data are presented as the mean ± standard error of the mean (SEM). *n* = 8−10 mice per group. Statistical analysis was done using one-way ANOVA followed by the Tukey post hoc test for C, E, G−I and two-way ANOVA followed by the Bonferroni post hoc test for A, B, D, F. $^{*}P < 0.05$; $^{**}P < 0.01$; $^{***}P < 0.001$ *vs* model

WIP improved hyperlipidemia and hepatic steatosis

Both WIP and inulin treatments showed no significant effects on dietary intake, body weight, and liver index (Figs. 3A−C). However, as to levels of serum total cholesterol (TC), triglycerides (TG) and low-density lipoprotein– cholesterol (LDL-C), WIP-treated mice exhibited markedly decrease in comparison with those of vehicle-treated group (Figs. 3D−F). In recent studies, a group of low-density-lipoprotein-cholesterol (LDL-C)-reducing agents have been confirmed to be effective in treating dyslipidemia in clinical trials [15-16]. Examination of hematoxylin-eosin (H&E)-stained sections of white adipose tissue (WAT) indicated an enlarged size of adipocytes in white adipose tissue of ob/ob mice. Oral treatment with WIP or inulin prevented adipocyte hypertrophy, indicating the improved adipose steatosis by WIP and inulin (Fig. 3G).

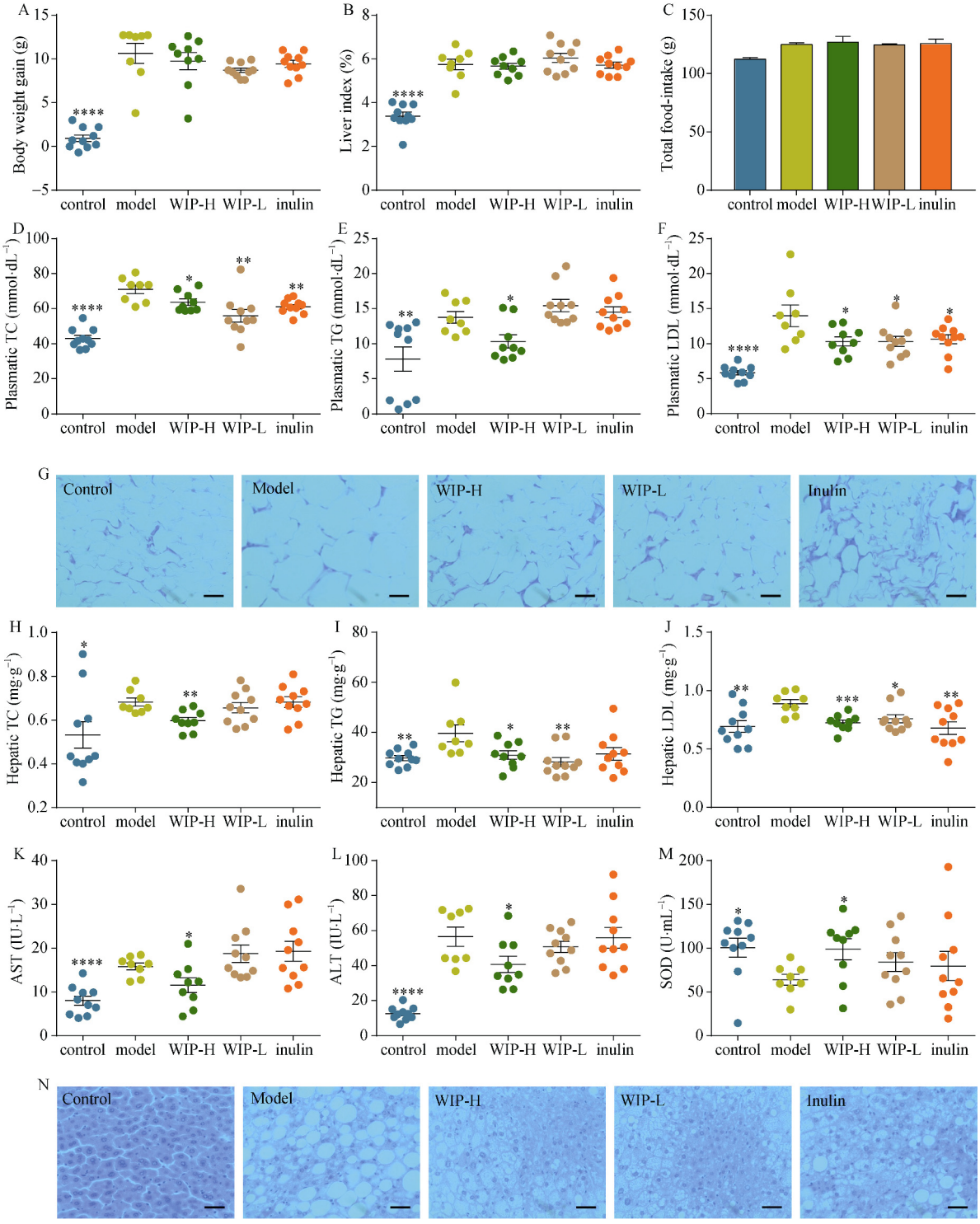

Fig. 3 WIP regulated lipid metabolism and ameliorate hepatic steatosis. (A) Body weight gain; (B) Liver index; (C) Total food intake; (D) Plasmatic total cholesterol; (E) Plasmatic triglyceride; (F) Plasmatic LDL-C; (G) Representative H&E-stained pictures and distribution of adipocyte size in WAT deposits (3 mice per group). Measurements were taken from distinct samples. Scale bars, 100 μm; (H) Hepatic total cholesterol; (I) Hepatic triglyceride; (J) Hepatic LDL-C; (K) Plasmatic AST; (L) Plasmatic ALT; (M) Plasmatic SOD; (N) Representative images of H&E staining of the liver (*n* = 3 mice per group). Scale bars, 100 μm. Measurements were taken from distinct samples. Control, C57B6/*J* mice control; Model, *ob/ob* model; WIP-H, WIP 1.0 g·kg^{-1}; WIP-L, WIP 0.5 g·kg^{-1}; Inulin, Inulin 5.0 g·kg^{-1}. Data are presented as the mean ± standard error of the mean (SEM). *n* = 8−10 mice per group. Statistical analysis was done using one-way ANOVA followed by the Tukey post hoc test. $^{*}P < 0.05$; $^{**}P < 0.01$; $^{***}P < 0.001$ *vs* model

Non-alcoholic fatty liver disease (NAFLD) is tightly associated with obesity and obesity-related disorders [17]. Next, we examined the effects of WIP on hepatic lipid metabolism and liver injury. We found that WIP treatment effectively reduced levels of TG, TC, and LDL-C in the livers of *ob/ob* mice (Figs. 3H−J) and decreased the activities of serum alanine aminotransferase (ALT), aspartate transaminase (AST), and increased the activities superoxide dismutase (SOD) (Figs 3K−M). AST and ALT are key clinical indicators for liver function, and the increase of AST and ALT indicates the damage of liver. SOD can eliminate oxygen free radical and relieve oxidative stress in the liver. In addition, WIP administered at 1.0 g·kg^{-1} and 0.5 g·kg^{-1} apparently reduced macrosteatosis and hepatocyte ballooning in the livers of *ob/ob* mice, as indicated by liver sections staining and microscopy observation (Fig. 3N). In contrast, *ob/ob* mice treated with inulin exerted less improvements on AST, ALT, SOD and hepatic macrosteatosis. These results support the effectiveness of WIP in reducing hepatic steatosis and liver injury.

Effects of WIP on gut microbiota composition

It is well-known that indigestible polysaccharides can serve as the main energy and carbon source for gut microbiota and subsequently benefit the growth of gut microbiota. To explore the effects of WIP on gut microbiota, we performed the high-throughput sequencing (Hiseq) of the V3-V4 hypervariable region of the 16S rRNA genes from the caecum contents of *ob/ob* mice. After removing unqualified sequences, an average of 525 operational taxonomic units (OTUs) per sample were obtained. Average of OTUs for each group and overlap were performed using Veen diagram (Fig. 4A).

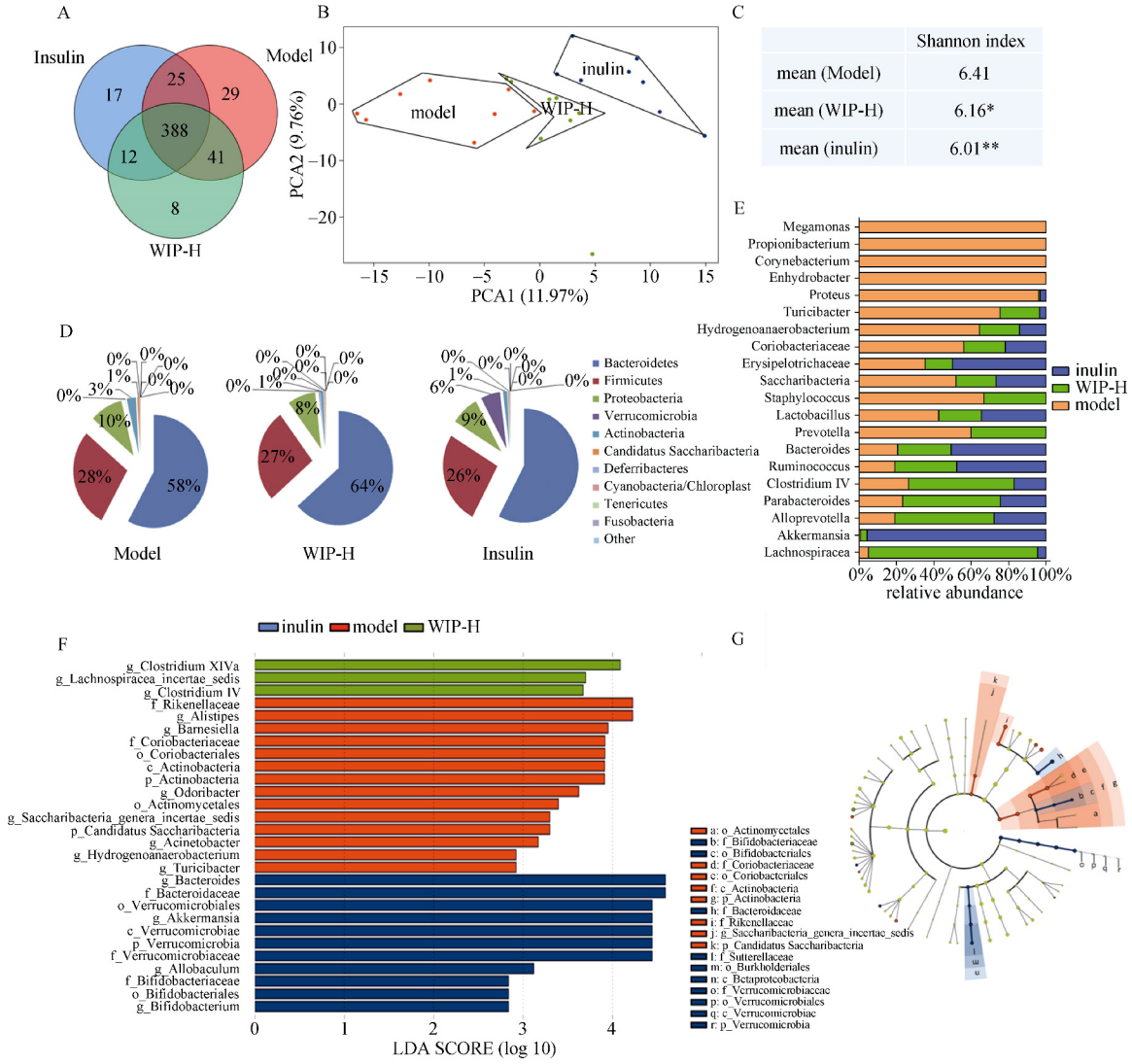

Fig. 4 Effects of WIP on gut microbiota composition. (A) OTU Venn diagram; (B) Principal component analysis based on OTU abundance; (C) Relative abundance of bacteria at the phylum level; (D) Shannon index; (E) The composition of the bacterial genera significantly affected by WIP treatment. Each column is set as 100% to illustrate the proportion of each genus among the different groups. (F, G) Taxonomic cladogram generated from LEfSe analysis of 16S rRNA gene sequences. Each circle's size is proportional to the taxon's abundance. Orange color represents enriched taxa in the model group; Green color represents enriched taxa in the WIP-treated group; Blue color indicates enriched taxa in the inulin-treated group. WIP-H, WIP 1.0 g·kg^{-1}; Inulin, Inulin 5.0 g·kg^{-1}

Principal component analysis on OTU level revealed that a distinct clustering of microbiota composition for each group (Fig. 4B). Meanwhile, Alpha-diversity was obviously decreased in both WIP and Inulin group as compared to the model group (Fig. 4C), which is in line with the phenomenon that less overall diversity implies better health [18]. The calculated relative abundance of bacteria at the phylum level was presented in Fig. 4D. WIP treated *ob/ob* mice significant raised the abundance of Bacteroidetes, whereas inulin increased the abundance of Verrucomicrobia, as compared to the vehicle treatment. Among the twenty genera significantly changed by WIP treatment, six SCFAs-production bacteria, *Lachnospiracea*, *Alloprevotella*, *Parabacteroides*, *Clostridum* IV, *Ruminococcus*, and *Bacteroides*, were markedly increased (Fig. 4E). Meanwhile, WIP administration induced a significantly decreased abundance of *Megamonas* and *Proteus* by 120- and 101-fold, respectively. *Megamonas*, and *Proteus* were reported to play important roles in pro-inflammatory responses or obesity [9, 19]. Further linear discriminant analysis (LDA) effect size (LEfSe) confirmed the increase of SCFA- producer *Lachnospiracea*, *Clostridium XIVa* and *Clostridium IV* in the WIP group. As for inulin treatment, a marked increase of *Akkermansia* and *bifidobacteriales* were observed, indicating a different regulation role on gut microbiota between WIP and inulin. Therefore, oral treatment with WIP greatly modulated the composition of gut microbiota.

WIP enhances butyrate production and maintains intestinal integrity

The diverse metabolites produced by gut microbiota, such as bile acid derivatives, SCFAs, amino acid derivatives, and lipopolysaccharide, have been identified as significant functional molecules linking gut microbiota with the physiopathology of host [20-22]. In line with the increased SCFA-producing bacteria, oral treatment with WIP significantly enhanced production of butyrate in mice fecal, as confirmed by GC-MS analysis (Fig. 5A). Butyrate, the product of polysaccharide fermentation by gut bacteria, plays significant physiological roles in stimulating mucin release, enhancing mRNA expression of mucosal integrity proteins and tight junction proteins [23]. Thus, we investigated the effects of WIP on mucosal barrier function in *ob/ob* mice. Results indicated that treatment with WIP at the dose of 1.0 g·kg^{-1} increased the mRNA expression of mucosal integrity proteins (Muc-5), and tight junction proteins (ZO-1 and Occludin) in the ileum (Figs. 5BD).

Metabolic endotoxemia, i.e. increased plasma lipopolysaccharide (LPS) levels, causes initiation of chronic low-grade inflammation (CLGI) that is known as a causal factor of obesity, insulin resistance, and hepatic steatosis [24-25]. LPS (a cell wall component of Gram-negative intestinal bacteria) can get into the circulation passing through the impaired barrier of the gut mucosa. According with the improved gut mucosa barrier function, we found that WIP treatment at the dose of 1.0 g·kg^{-1} led to 10.9 % reduction of plasma LPS in *ob/ob* mice (Fig. 5E) in comparison with that of vehicle-treated mice. Meanwhile, WIP significantly decreased the level of TNF-α, an important inflammatory factor stimulated by LPS (Fig. 5F). The elevated TNF-α in the plasma has been recognized as an important risk factor for metabolic syndrome [26-27].

Butyrate also participates in the maintenance of gut homeostasis [28]. It has been demonstrated that butyrate controls dysbiotic expansion of facultative anaerobic bacteria by reducing oxygen or nitrate supply to these bacteria through butyrate-activated PPAR-γsignaling [9]. The activation of epithelial PPAR-γ signaling by butyrate increases β-oxidation of fatty acids and lowers the release of nitrate. We found that treatment with WIP upregulated mRNA expression of *pparg* and significantly decreased nitrate levels in the colonic lumen (Figs. 5G and H). Thus, the enhanced production of butyrate by WIP has two aspects of benefits, including the improvement of gut barrier function and the prevention of Gram-negative *Proteus* (Proteobacteria, Enterobacteriaceae). Both benefits from butyrate led to the reduction of endoxemia and subsequently ameliorated the metabolic disorders.

Fecal transplantation ameliorates hyperglycemia and lipid metabolism

To further confirm the role of gut microbiota in mediating the effects of WIP, we transferred the microbiota of WIP-treated mice to *ob/ob* mice, followed by examination of metabolic syndrome related indexes. In comparison with vehicle group, transplantation with the feces of WIP-treated group markedly decreased free-diet blood glucose, plasm TC and TG, increased insulin sensitivity index (Fig. 6A−D). These results further confirmed that gut microbiota plays an important and causative role for the beneficial efficacies of WIP in improving glucose and lipid homeostasis.

Discussion

Water-soluble polysaccharides from the *P. cocos* have been well demonstrated with various bioactivities, including diuretic activity, anti-oxidation, anti-apoptosis, anti-cancer, anti-nephritis, and anti-angiogenesis [29]. Four antioxidant water-soluble polysaccharides with the molecular weight of 2.15×10^4 Da, 2.12×10^4 Da, 1.06×10^4 Da and 1.51×10^4 Da were reported from *P. cocos* [30]. Bian *et al*. reported water-soluble pachyman with anticancer activity from *P. cocos* [31]. It was found that water insoluble soluble polysaccharides took up 70% of the dry weight of sclerotium [32]. There is no report on the hypoglycemic and hypolipidemic activities of water insoluble polysaccharides from the sclerotium of *P. cocos*. In this study, we investigated the beneficial effects of a water insoluble soluble polysaccharide from the sclerotium of *P. cocos* on obesity-related metabolic disorders. The water insoluble polysaccharide (WIP) of *P. cocos* was identified as a main chain of 1, 3-β-D-glucan with an average Mw of 448.6×10^4 Da. WIP of *P. cocos* displayed multiple benefits in reducing hyperglycemia and hyperlipidemia, and reducing hepatic steatosis on obese mice. In contrast with insulin, WIP showed

better effects in improving the glucose tolerance and insulin resistance, reducing levels of the plasma and heptatic TG, the plasma TC, the serum ALT and AST, and increasing the level of SOD at the dose of 1.0 g·kg^{-1}.

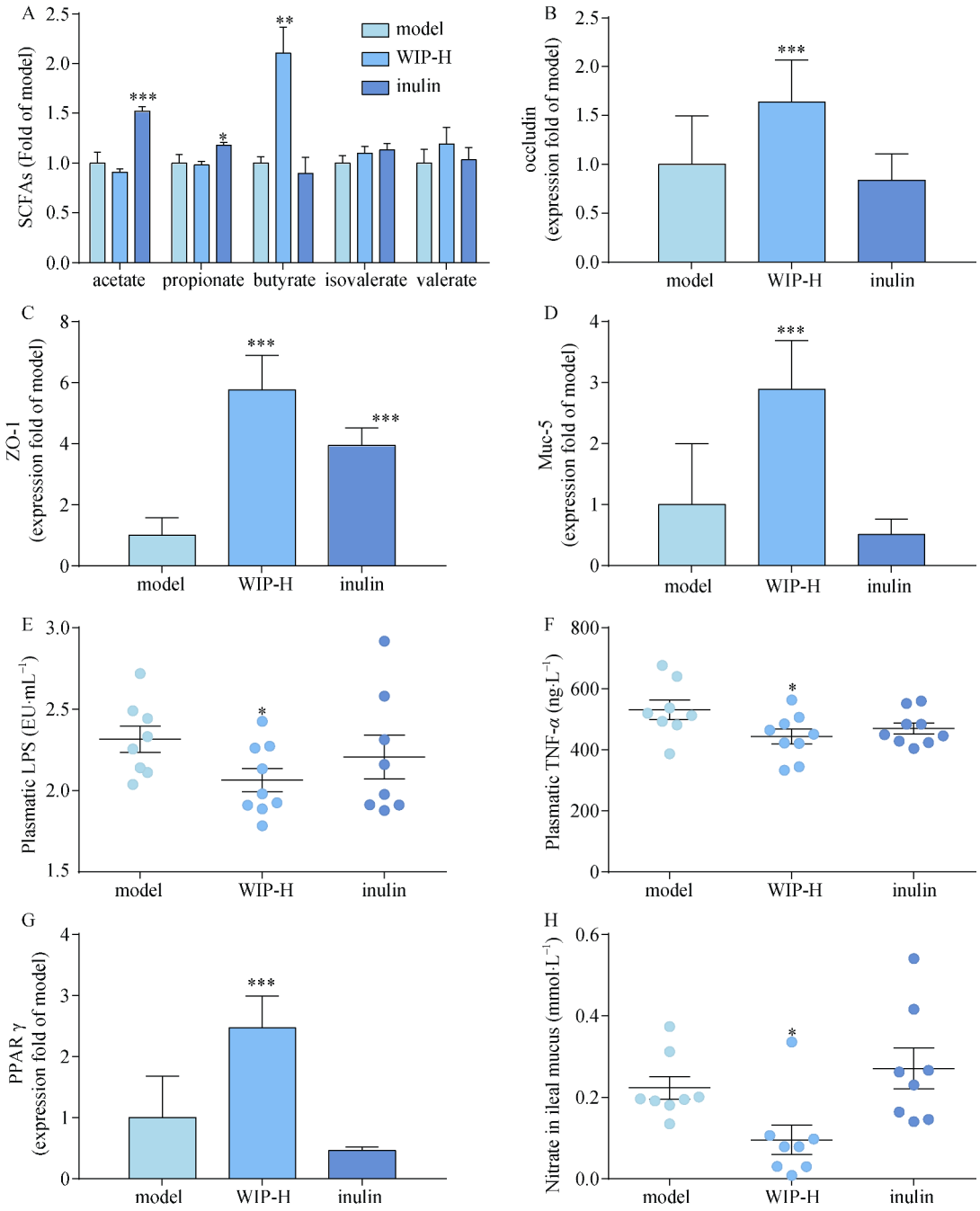

Fig. 5 WIP enhance butyrate production and maintain intestinal integrity. (A) Levels of short chain fatty acids (SCFAs) in the fecal samples; The relative mRNA expression level of muc-5 (B) occludin (C) Zonula occludens-1 (ZO-1) (D) in ileum, (E) Plasmatic levels of LPS; (F) Plasmatic levels of TNF*α* by ELISA; (G) The relative mRNA expression level of PPAR-*γ* in ileum, (H) Concentration of nitrate in ileal mucus. WIP-H, WIP 1.0 g·kg^{-1}; Inulin, Inulin 5.0 g·kg^{-1}. Data are presented as the mean ± standard error of the mean (SEM). Statistical analysis was done using one-way ANOVA followed by the Tukey post hoc test. $^{*}P < 0.05$; $^{**}P < 0.01$; $^{***}P < 0.001$ *vs* model

Recent evidence suggests that the intestinal microbiota composition is closely associated with occurrence and development of metabolic syndrome. A prebiotic is food ingredient that is not digested in the digestive tract but fermented by gut microbiota. Prebiotics possess the ability of promoting the growth or activity of specific gut microbes that have the

potential to improve human and animal health or reduce risk of diseases [33]. Effects of prebiotics have been claimed from infants to the elder. Over the past ten years, a number of prebiotics have been reported to improve metabolic diseases. Polysaccharide from *Plantago asiatica* L. significantly increased *Bacteroides vulgatus*, *Lactobacillus fermentum*, *Prevotella loescheii* and *Bacteroides vulgates* to attenuate hyperglycemia and hyperlipidemia in type 2 diabetes [34]. Diet supplement of oligofructose significantly increased the abundance of *Bifidobacterium* spp. and reduced fat-mass development, oxidative stress, and low-grade inflammation in o*b/ob* mice [35]. Fuzhuan brick tea polysaccharides increased the abundance of *Erysipelotrichaceae*, *Coriobacteriaceae* and *Streptococcaceae* and attenuated metabolic syndrome in HFD-induced mice [36]. In this study, the results of 16s sequencing showed that inulin mainly increased *Akkermansia* and *bifidobacteriales*. However, WIP mainly increased the abundant of *Lachnospiracea, Clostridium XIVa and Clostridium IV*. The abundance of *Clostridium XIVa and Clostridium IV* has been demonstrated to be negatively correlated with liver steatosis [37]. The different modulation effects on gut microbiota between WIP and inulin may partly explain their difference on the regulation of obese-related dysfunctions.

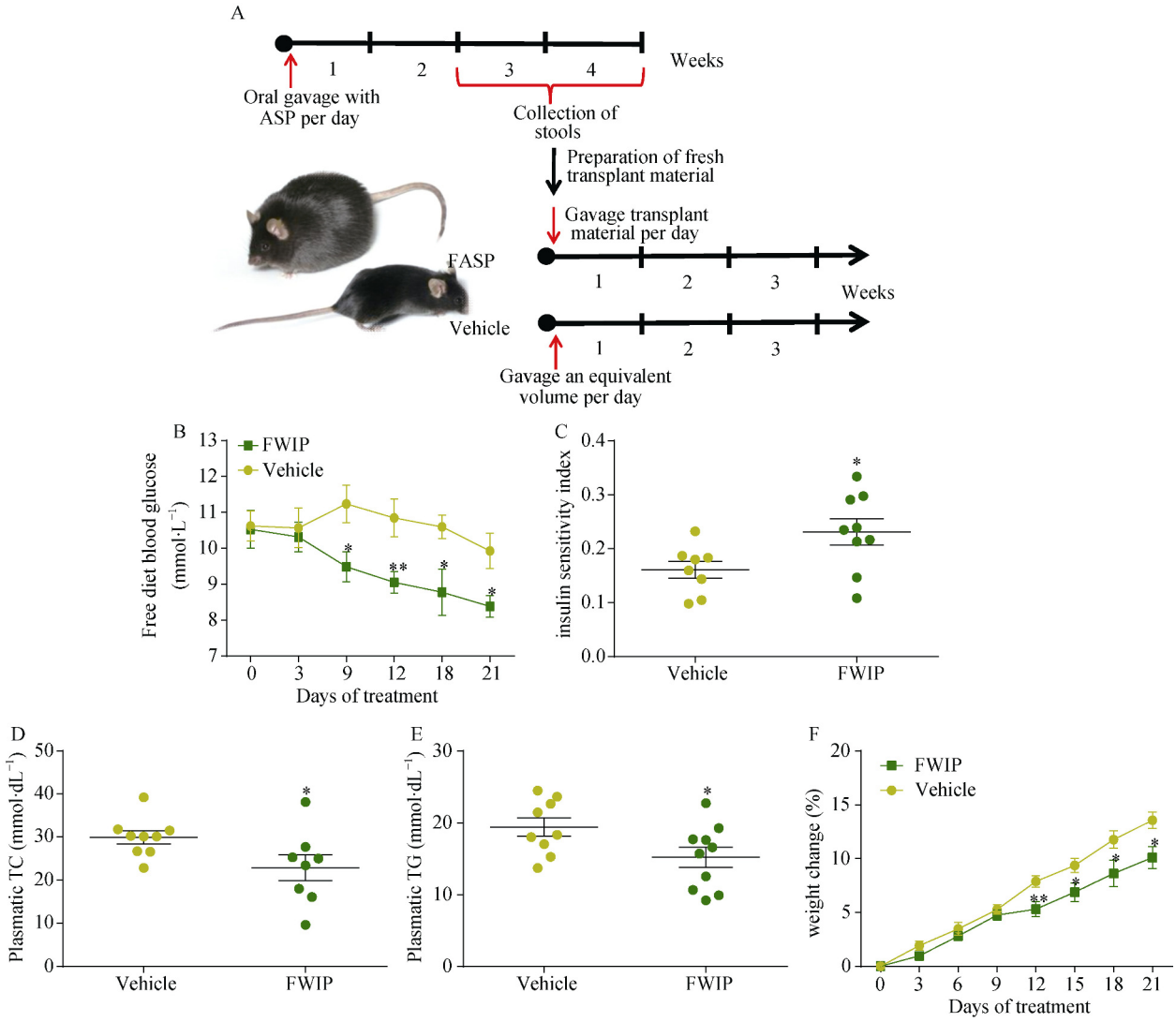

Fig. 6 Fecal transplantation ameliorates hyperglycemia and lipid metabolism. (A) Experimental design (B) Free diet glucose, (C) Insulin sensitivity index, (D) Plasmatic total cholesterol, (E) Plasmatic triglyceride, (F) Weight change. FWIP, the fecal of WIP treated mice. Data are presented as the mean ± standard error of the mean (SEM). Statistical analysis was done using one-way ANOVA followed by the Tukey post hoc test. $^{*}P < 0.05$; $^{**}P < 0.01$; $^{***}P < 0.001$ *vs* model

The main products of prebiotics fermented by gut microbiota are short-chain fatty acids, in particular, acetate, propionate, and butyrate. In consistence with the increased abundance of butyrate-producing bacteria *Lachnospiracea*, *Clostridium* XIVa and *Clostridium* IV, WIP treatment greatly enhanced the level of butyrate in feces. Butyrate-producing bacteria represent

a functional group rather than a coherent phylogenetic group within the microbial community of the human large intestine. Butyrate plays a key role in maintaining human gut health, serving as the major source of energy to the colonic mucosa and an important regulator of gene expression, inflammation, differentiation and apoptosis in host cells [38]. Butyrate also contributes to the maintenance of gut homeostasis through activating PPAR-γ signaling pathway to control the oxygen and nitrate supply to pro-inflammatory bacteria [9]. In line with the higher level of butyrate in the feces, WIP treatment significantly increased the expression of ileum PPAR-γ and activated the PPAR-γ signaling. Previous studies have indicated that obesity-induced gut dysbiosis impairs intestinal integrity, leading to the release of LPS into blood [39-40]. The increase of LPS in the circulation induces insulin resistance and inflammation in obese mice. It has been demonstrated that butyrate in gut can promote the development of the intestinal barrier [21]. Oral treatment with WIP beneficially recovered the gut integrity through upregulating the expression of mucosal integrity proteins (Muc-5) and tight junction proteins (ZO-1 and Occludin) in the ileum, which is partly due to the increased butyrate in gut by WIP.

In conclusion, we have for the first time demonstrated the benefits of WIP from the sclerotium of *P. cocos* against metabolic dysfunctions, including hyperglycemia, hyperlipidemia and hepatic steatosis. Modulation of gut microbiota, especially the increase of butyrate-producing bacteria, has been confirmed as one of important mechanism of WIP for its metabolic benefits. Our findings implicate the potential of the water insoluble polysaccharide from *P. cocos* as a prebiotic for the prevention and cure of metabolic diseases and elucidate new mechanism for the efficacies of this traditional herbal medicine on regulation of glucose and lipid metabolism.

References

[1] Blandino G, Inturri R, Lazzara F, *et al*. Impact of gut microbiota on diabetes mellitus [J]. *Diabetes Metab*, 2016, **42**(5): 303-315.

[2] Kootte RS, Vrieze A, Holleman F, *et al*. The therapeutic potential of manipulating gut microbiota in obesity and type 2 diabetes mellitus [J]. *Diabetes Obes Metab*, 2012, **14**(2): 112-120.

[3] Li X, Watanabe K, Kimura I. Gut microbiota dysbiosis drives and implies novel therapeutic strategies for diabetes mellitus and related metabolic diseases [J]. *Front Immunol*, 2017, **8**(1882): 1-7.

[4] Mulders RJ, de Git KCG, Schele E, *et al*. Microbiota in obesity: interactions with enteroendocrine, immune and central nervous systems [J]. *Obes Rev*, 2018, **19**(4): 435-451

[5] Chang CJ, Lin CS, Lu CC, *et al*. *Ganoderma lucidum* reduces obesity in mice by modulating the composition of the gut microbiota. *Nat Commun*, 2015, **6**(7489): 1-17.

[6] Hu Y, Teng C, Yu S, *et al*. *Inonotus obliquus* polysaccharide regulates gut microbiota of chronic pancreatitis in mice [J]. *AMB Express*, 2017, **7**(39): 1-11.

[7] Chen DL, Yang X, Zheng CQ, *et al*. Extracts from *Hericium erinaceus* relieve inflammatory bowel disease by regulating immunity and gut microbiota [J]. *Oncotarget*, 2017, **8**(49); 85838-85857.

[8] Yang XB, Zhao Y, Wang QW, *et al*. Analysis of the monosaccharide components in Angelica polysaccharides by high performance liquid chromatography [J]. *Anal Sci*, 2005, **21**(10): 1177-1180.

[9] Byndloss MX, Olsan EE, Rivera-Chavez F, *et al*. Microbiota-activated PPAR-gamma signaling inhibits dysbiotic Enterobacteriaceae expansion [J]. *Science*, 2017, **357**(6351): 570-575.

[10] Wang K, Bao L, Zhou, N, *et al*. Structural modification of natural product ganomycin I leading to discovery of a alpha-glucosidase and HMG-CoA reductase dual inhibitor improving obesity and metabolic dysfunction *in vivo* [J]. *J Med Chem*, 2018, **61**(8): 3609-3625.

[11] Cheng HN, Neiss TG. Solution NMR Spectroscopy of Food Polysaccharides [J]. *Polym Rev*, 2012, **52**(2): 81-114.

[12] Kumar SA, Ward LC, Brown L. Inulin oligofructose attenuates metabolic syndrome in high-carbohydrate, high-fat diet-fed rats [J]. *Brit J Nutr*, 2016, **116**(9): 1502-1511.

[13] Liu F, Prabhakar M, Ju J, *et al*. Effect of insulin-type fructans on blood lipid profile and glucose level: a systematic review and meta-analysis of randomized controlled trials [J]. *Eur J Clin Nut*, 2017, **71**(1): 9-20.

[14] Stratton IM, Adler AI, Neil HAW, *et al*. Association of glycaemia with macrovascular and microvascular complications of type 2 diabetes (UKPDS 35): prospective observational study [J]. *Brit Med J*, 2000, **321**(7258): 405-412.

[15] Rader DJ. New therapeutic approaches to the treatment of dyslipidemia [J]. *Cell Metab*, 2016, **23**(3): 405-412.

[16] Stein EA, Mellis S, Yancopoulos GD, *et al*. Effect of a monoclonal antibody to PCSK9 on LDL cholesterol [J]. *N Engl J Med*. 2012, **366**(12), 1108-1118.

[17] Tarantino G, Saldalamacchia G, Conca P, *et al*. Non-alcoholic fatty liver disease: further expression of the metabolic syndrome [J]. *J Gastroen Hepatol*, 2007, **22**(3): 293-303.

[18] Zhao L, Zhang F, Ding X, *et al*. Gut bacteria selectively promoted by dietary fibers alleviate type 2 diabetes [J]. *Science*, 2018, **359**(6380): 1151-1156.

[19] Chiu CM, Huang WC, Weng SL, *et al*. Systematic analysis of the association between gut flora and obesity through high-throughput sequencing and bioinformatics approaches [J]. *Biomed Res Int*, 2014, **2014**(906168): 1-10.

[20] Koh A, De Vadder F, Kovatcheva-Datchary P, *et al*. From dietary fiber to host physiology: short-chain fatty acids as key bacterial metabolites [J]. *Cell*, 2016, **165**(6): 1332-1345.

[21] Wahlstrom A, Sayin SI, Marschall HU, *et al*. Intestinal crosstalk between bile acids and microbiota and its impact on host metabolism [J]. *Cell Metab*, 2016, **24**(1): 41-50.

[22] Lee CC, Watkins SM, Lorenzo C, *et al*. Branched-chain amino acids and insulin metabolism: the insulin resistance atherosclerosis study (IRAS) [J]. *Diabetes Care*, 2016, **39**(4): 582-588.

[23] Ploger S, Stumpff F, Penner GB, *et al*. Microbial butyrate and its role for barrier function in the gastrointestinal tract [J]. *Ann Ny Acad Sci*, 2012, **1258**: 52-59.

[24] Hotamisligil GS. Inflammation and metabolic disorders [J]. *Nature*, 2006, **444**(7121): 860-867.

[25] Mehta NN, McGillicuddy FC, Anderson PD, *et al*. Experimental endotoxemia induces adipose inflammation and insulin resis-

tance in humans [J]. *Diabetes*, 2010, **59**(1): 172-181.
[26] Hu FB, Meigs JB, Li TY, *et al*. Inflammatory markers and risk of developing type 2 diabetes in women [J]. *Diabetes*, 2004, **53**(3): 693-700.
[27] Koh KK, Han SH, Quon MJ. Inflammatory markers and the metabolic syndrome-insights from therapeutic interventions [J]. *J Am Coll Cardiol*, 2005, **46**(11): 1978-1985.
[28] Leonel AJ, Alvarez-Leite JI. Butyrate: implications for intestinal function [J]. *Curr Opin Clin Nutr*, 2012, **15**(5): 474-479.
[29] Jia XJ, Ma LS, Li P, *et al*. Prospects of *Poria cocos* polysaccharides: isolation process, structural features and bioactivities [J]. *Trends Food Sci Tech*, 2016, **54**: 52-62.
[30] Wang N, Zhang Y, Wang X, *et al*. Antioxidant property of water-soluble polysaccharides from *Poria cocos* Wolf using different extraction methods [J]. *Int J Biol Macromol*, 2016, **83**: 103-110.
[31] Bian C, Xie NN, Chen FS. Preparation of bioactive water-soluble pachyman hydrolyzed from sclerotial polysaccharides of *Poria cocos* by hydrolase [J]. *Polym J*, 2010, **42**(3): 256-260.
[32] Kang YZ, Wang WH. Determination of Water-soluble Polysaccharide and alkali-soluble polysaccharide in *Poria* by near infrared spectroscopy [J]. *Chin J of Exp Tradit Med Form*, 2016, **22**(24): 80-83.
[33] Gibson GR, Hutkins R, Sanders ME, *et al*. The international scientific association for probiotics and prebiotics (ISAPP) consensus statement on the definition and scope of prebiotics [J]. *Nat Rev Gastro Hepat*, 2017, **14**(8): 491-502.
[34] Nie Q, Hu J, Gao H, *et al*. Polysaccharide from Plantago asiatica L. attenuates hyperglycemia, hyperlipidemia and affects colon microbiota in type 2 diabetic rats [J]. *Food Hydrocolloids*, 2019, **86**(SI): 34-42.
[35] Everard A, Lazarevic V, Derrien M, *et al*. Responses of gut microbiota and glucose and lipid metabolism to prebiotics in genetic obese and diet-induced leptin-resistant mice [J]. *Diabetes*, 2011, **60**(11): 2775-2786.
[36] Chen G, Xie M, Wan P, *et al*. Fuzhuan brick tea polysaccharides attenuate metabolic syndrome in high-fat diet induced mice in association with modulation in the gut microbiota [J]. *J Agric Food Chem*, 2018, **66**(11): 2783-2795.
[37] Neyrinck AM, Possemiers S, Verstraete W, *et al*. Dietary modulation of *clostridial* cluster XIVa gut bacteria (*Roseburia spp*) by chitin-glucan fiber improves host metabolic alterations induced by high-fat diet in mice [J]. *J Nutr Biochem*, 2012, **23**(1): 51-59.
[38] Louis P, Flint HJ. Diversity, metabolism and microbial ecology of butyrate-producing bacteria from the human large intestine [J]. *Fems Microbiol Lett*, 2009, **294**(1): 1-8.
[39] Cani PD, Bibiloni R, Knauf C, *et al*. Changes in gut microbiota control metabolic endotoxemia-induced inflammation in high-fat diet-induced obesity and diabetes in mice [J]. *Diabetes*, 2008, **57**(6): 1470-1481.
[40] Cani PD, Amar J, Iglesias MA, *et al*. Metabolic endotoxemia initiates obesity and insulin resistance [J]. *Diabetes*, 2007, **56**(7): 1761-177.

Cite this article as: SUN Shan-Shan, WANG Kai, MA Ke, BAO Li, LIU Hong-Wei. An insoluble polysaccharide from the sclerotium of *Poria cocos* improves hyperglycemia, hyperlipidemia and hepatic steatosis in *ob/ob* mice *via* modulation of gut microbiota [J]. *Chin J Nat Med*, 2019, **17**(1): 3-14.